Global decoupling of functional and phylogenetic diversity in plant communities

Georg J. A. Hähn[1,2,3,*], Gabriella Damasceno[2,1], Esteban Alvarez-Davila[4], Isabelle Aubin[5], Marijn Bauters[6], Erwin Bergmeier[7], Idoia Biurrun[8], Anne D. Bjorkman[9,10], Gianmaria Bonari[11], Zoltán Botta-Dukát[12], Juan A. Campos[8], Andraž Čarni[13,14], Milan Chytrý[15], Renata Ćušterevska[16], André Luís de Gasper[17], Michele De Sanctis[18], Jürgen Dengler[19], Jiri Dolezal[20], Mohamed A. El-Sheikh[21], Manfred Finckh[22], Antonio Galán-de-Mera[23], Emmanuel Garbolino[24], Hamid Gholizadeh[11], Valentin Golub[25], Sylvia Haider[26], Mohamed Z. Hatim[27], Bruno Hérault[28,29], Jürgen Homeier[30], Ute Jandt[1,2], Florian Jansen[31], Anke Jentsch[32], Jens Kattge[33,2], Michael Kessler[34], Larisa Khanina[35], Holger Kreft[36], Filip Küzmič[13], Jonathan Lenoir[37], Jesper Erenskjold Moeslund[38], Ladislav Mucina[39,40], Alireza Naqinezhad[41], Jalil Noroozi[42], Aaron Pérez-Haase[43], Oliver L. Phillips[44], Valério D. Pillar[45], Gonzalo Rivas-Torres[46], Eszter Ruprecht[47], Brody Sandel[48], Marco Schmidt[49], Ute Schmiedel[50], Stefan Schnitzer[51], Franziska Schrodt[52], Urban Šilc[13], Ben Sparrow[53], Maria Sporbert[1,2], Zvjezdana Stančić[54], Ben Strohbach[55], Jens-Christian Svenning[56], Cindy Q. Tang[57], Zhiyao Tang[58], Alexander Christian Vibrans[59], Cyrille Violle[60], Donald Waller[61], Desalegn Wana[62], Hua-Feng Wang[63], Timothy Whitfeld[64], Georg Zizka[65], Francesco Maria Sabatini[3,66,†] & Helge Bruelheide[1,2,†]

[*] Corresponding author: georg.haehn@idiv.de

[†] These authors jointly supervised this work

[1] Martin Luther University Halle-Wittenberg, Institute of Biology / Geobotany and Botanical Garden, Am Kirchtor 1, 06108 Halle, Germany

[2] German Centre for Integrative Biodiversity Research (iDiv) Halle-Jena-Leipzig, Puschstrasse 4, Leipzig, 04103, Germany

[3] University of Bologna, Department of Biological, Geological and Environmental Sciences, Via Irnerio 42, Bologna, 40126, Italy

[4] Universidad Nacional Abierta y a Distancia (Colombia), Escuela ECAPMA, Street 14 Sur # 14-23, Bogotá, Postal Code 111511, Colombia

[5] Canadian Forest Service, Great Lakes Forestry Centre, 1219 Queen St. East, Sault Ste Marie, ON, P6A 2E5, Canada

[6] Ghent University, Department of Environment, Coupure Links 653, 9000 Gent, Belgium

[7] University of Göttingen, Deptartment of Vegetation & Phytodiversity Analysis, Untere Karspüle 2, Göttingen, 37073, Germany
[8] University of the Basque Country UPV/EHU, Department of Plant Biology and Ecology, Apdo. 644, 48080, Bilbao, Spain
[9] University of Gothenburg, Biological & Environmental Sciences, Box 463, 40530, Gothenburg, Sweden
[10] Gothenburg Global Biodiversity Centre, Box 463, 40530, Gothenburg, Sweden
[11] University of Siena, Department of Life Sciences, Via P.A. Mattioli 4, 53100, Siena, Italy
[12] Centre for Ecological Research, Institute of Ecology and Botany, Alkotmány 2-4, Vácrátót, 2163, Hungary
[13] Research Centre of the Slovenian Academy of Sciences and Arts, Jovan Hadži Institute of Biology, Novi trg 2, SI 1000 Ljubljana, Slovenia
[14] University of Nova Gorica, School for Viticulture and Enology, Vipavska cesta 13, 5000 Nova Gorica, Slovenia
[15] Masaryk University, Faculty of Science, Department of Botany and Zoology, Kotlářská 2, 611 37 Brno, Czech Republic
[16] University of Ss. Cyril and Methodius, Faculty of Natural Sciences and Mathematics, Institute of Biology, Arhimedova Str. 3, 1000, Skopje, North Macedonia
[17] Universidade Regional de Blumenau, Rua Antonio da Veiga, 140, 89030903, Blumenau, Santa Catarina, Brazil
[18] Sapienza University of Rome, Department of Environmental Biology, P.le Aldo Moro 5, Rome, 00185, Italy
[19] Zurich University of Applied Sciences (ZHAW), Wädenswil, Switzerland
[20] Czech Academy of Science, Institute of Botany, Dukelská 135, 379 01 Trebon, Czechia
[21] King Saud University, College of Science, Botany and Microbiology Department, P.O. Box 2455, Riyadh 11451, Saudi Arabia
[22] University of Hamburg, Institute of Plant Science and Microbiology, Ohnhorststr., 18, Hamburg, 22609, Germany
[23]Universidad San Pablo-CEU, CEU Universities, Botany Lab, Carretera de Boadilla Km 5,300, 28660- Boadilla del Monte, Madrid, Spain
[24] MINES Paris PSL - ISIGE, 35 rue Saint-Honoré, 77300 Fontainebleau, France
[25] Samara Federal Research Scientific Center, Institute of Ecology of the Volga River Basin,

Komzina 10 Togliatti, 445003, Russia
[26] Leuphana University of Lüneburg, School of Sustainability, Institute of Ecology, Universitätsallee 1, 21335 Lüneburg, Germany
[27] Wageningen University, Plant Ecology and Nature Conservation Group, Environmental Sciences Department, P.O. Box Postbus 47, Droevendaalsesteeg 3, 6700 AA, Wageningen, The Netherlands
[28] CIRAD, UPR Forêts et Sociétés, Campus de Baillarguet, F-34398 Montpellier, France
[29] University Montpellier, CIRAD, Forêts et Sociétés, Campus de Baillarguet, F-34398 Montpellier, France
[30] HAWK Goettingen, Resource Management, Daimlerstraße 2, 37075 Goettingen, Germany
[31] University of Rostock, Justus-von-Liebig-Weg 6, 18059 Rostock, Germany
[32] University of Bayreuth, Bayreuth Center of Ecology and Evironmental Research, Department of Disturbance Ecology, Bayreuth, Germany
[33] Max Planck Institute for Biogeochemistry, Hans Knöll Str. 10, 07745 Jena, Germany
[34] University of Zurich, Systematic and Evolutionary Botany, Zollikerstrasse 107, CH-8008 Zurich, Switzerland
[35] IMPB RAS, Branch of the M.V. Keldysh IAM RAS, 1 Prof. Vitkevicha Str., Pushchino, 142290, Russia
[36] University of Göttingen, Department of Biodiversity, Macroecology & Biogeography, Büsgenweg 1, 37077 Göttingen, Germany
[37] UMR CNRS 7058 Ecologie et Dynamique des Systèmes Anthropisés (EDYSAN), Université de Picardie Jules Verne, 1 rue des Louvels, 80000 Amiens, France
[38] Aarhus University, Department of Ecoscience, C. F. Møllers Allé 6-8, DK-8000, Aarhus C, Denmark
[39] Murdoch University, Harry Butler Institute, 90 South Street, Murdoch 6150, Perth, Western Australia, Australia
[40] Stellenbosch University, Department of Geography & Environmental Studies, Private Bag X1, 7602 Matieland, Stellenbosch, South Africa
[41] University of Derby, Department of Environmental Sciences, College of Science and Engineering, Kedleston Road, Derby, United Kingdom
[42] University of Vienna, Department of Botany and Biodiversity Research, Rennweg 14, Vienna, 1030, Austria

[43] Universitat de Barcelona, Departament de Biologia Evolutiva, Ecologia i Ciències Ambientals, Institut de Recerca de la Biodiversitat (IRBio), Av. Diagonal 643, Barcelona, 08036, Spain
[44] University of Leeds, Leeds LS2 9JT, United Kingdom
[45] Universidade Federal do Rio Grande do Sul, Department of Ecology, Porto Alegre, RS, 91501-970, Brazil
[46] Estación de Biodiversidad Tiputini, Universidad San Francisco de Quito USFQ, Colegio de Ciencias Biológicas y Ambientales, Diego de Robles sn e Interoceanica, Quito, Ecuador
[47] Babeș-Bolyai University, Faculty of Biology and Geology, Hungarian Department of Biology and Ecology, Republicii street 42., 400015 Cluj-Napoca, Romania
[48] Santa Clara University, Department of Biology, 500 El Camino Real, Santa Clara CA, 95053, USA
[49] Palmengarten der Stadt Frankfurt am Main, Wissenschaft, Siesmayerstraße 61, 60323 Frankfurt am Main, Germany
[50] University of Hamburg, Institute of Plant Science and Microbiology, Ohnhorststraße 18, 22609 Hamburg, Germany
[51] Marquette University, PO Box 1881, Milwaukee WI 53202
[52] University of Nottingham, University Park, Nottingham, NG7 2RD, United Kingdom
[53] University of Adelaide, TERN, The School of Biological Sciences, Waite Campus, PMB 1, Glen Osmond, SA, 5064, Australia
[54] University of Zagreb, Faculty of Geotechnical Engineering, Hallerova aleja 7, HR-42000 Varaždin, Croatia
[55] Namibia University of Science and Technology, Biodiversity Research Center, Faculty of Health, Natural Resources and Applied Sciences, 13 Jackson Kaujeua street, Windhoek, Namibia
[56] Aarhus University, Department of Biology, Center for Ecological Dynamics in a Novel Biosphere (ECONOVO), Ny Munkegade 114, DK-8000 Aarhus C, Denmark
[57] Yunnan University, Institute of Ecology and Geobotany, College of Ecology and Environmental Science, Building Shixun, Chenggong Campus, Dongwaihuan South Road, University Town, Chenggong New District, Kunming, Yunnan 650504, China
[58] Peking University, Department of Ecology, College of Urban and Environmental Sciences, Yiheyuan Road 5, Haidian, Beijing 100871, China

[59] Universidade Regional de Blumenau (FURB), Rua São Paulo, 3250, Blumenau-Santa Catarina Zipcode 89030-000, Brazil
[60] CEFE, Univ Montpellier, CNRS, EPHE, IRD, Campus CNRS, 1919 route de Mende, 34293 Montpellier, France
[61] University of Wisconsin - Madison, Botany, 2150 West Lawn Ave, Madison WI, 53711, USA
[62] Addis Ababa University, Department of Geography & Environmental Studies, Bole street, Addis Ababa, P.O. Box 150178, Ethiopia
[63] Hainan University, Sanya Nanfan Research Institute, Sanya, 572500, Hainan, China
[64] University of Minnesota, Bell Musuem, 1479 Gortner Avenue, St. Paul, MN 55108, USA
[65] Senckenberg Research Institute and Natural History Museum Frankfurt and Goethe University, Department Botany and Molecular Evolution, Senckenberganlage 25, 60325 Frankfurt/Main, Germany
[66] Faculty of Forestry and Wood Sciences, Czech University of Life Sciences Prague, 165 00 Praha, Czech Republic

Abstract

Plant communities are composed of species that differ both in functional traits and evolutionary histories. As species' functional traits partly result from their individual evolutionary history, we expect the functional diversity of communities to increase with increasing phylogenetic diversity. This expectation has only been tested at local scales and generally for specific growth forms or specific habitat types, e.g., grasslands. Here, we compare standardized effect sizes for functional and phylogenetic diversity among 1,781,836 vegetation plots using the global sPlot database. In contrast to expectations, we find functional diversity and phylogenetic diversity to be only weakly and negatively correlated, implying a decoupling between these two facets of diversity. While phylogenetic diversity is higher in forests and reflects recent climatic conditions (1981 to 2010), functional diversity tends to reflect recent and past climatic conditions (21,000 years ago). The independent nature of functional and phylogenetic diversity makes it crucial to consider both aspects of diversity when analyzing ecosystem functioning and prioritizing conservation efforts.

Introduction

Climate change and biodiversity loss are pressing environmental issues, with rising temperatures and shifting precipitation patterns increasingly driving plant species extinctions[1]. These changes have significant implications for ecosystems and human societies alike, with impacts ranging from altered agricultural yields to increased risk of natural disasters[2–4]. To understand and mitigate the effects of climate change and biodiversity loss, it is crucial to determine how plant species assemble into communities and how these communities respond to changing environmental and climatic conditions[5,6]. To do this, we need to understand the underlying mechanisms of plant community assembly and how environmental conditions, species' functional traits and evolutionary histories interact to mediate these mechanisms[7].

Community assembly reflects several processes that can reinforce or oppose each other[8]. On the one hand, environmental filters tend to favor similar phenotypic traits generating clustering within a community[9,10]. On the other hand, biotic interactions like competitive exclusion often limit how similar phenotypes can be as species with different traits coexist more readily, fostering trait divergence[11,12]. Attributing convergence or divergence to specific mechanisms is difficult, however, competitive exclusion can also generate convergence when other traits are associated with low competitive abilities[8]. Likewise, divergence can stem from habitat filtering when traits become correlated with distinct sets of environmental controls[13] or when interacting environmental factors select for resident species[14]. Whatever the underlying mechanism, species functional traits play an important role in community assembly while also reflecting how species evolved within specific environments. In other words, functional traits reflect past selection and are often conserved within phylogenetic lineages. Species closely related on the evolutionary tree are thus more likely to share similar traits compared to less closely related species. Depending on the pace of evolution, specific traits can be more or less conserved on the phylogenetic tree[15,16]. Indices based on Brownian motion models of trait evolution like Blomberg`s $K$ and Pagel`s λ[17,18] allow us to test whether traits are phylogenetically conserved. These indices are based on correlations between species' distances in trait values and distances along their shared phylogeny[7,19,20].

When species within a community share similar traits, the community is said to show phenotypic clustering, reducing functional diversity (FD). Phenotypic clustering can be associated with two patterns, either a combination of phylogenetic clustering with trait conservatism (*Fig. 1*, bottom left) or a combination of phylogenetic dispersion with trait convergence (*Fig. 1*, bottom right)[7,15,21]. In the former case, there is a positive covariation between phylogenetic and functional distances, which is why we call the resulting diversity metrics coupled. In the latter case, the phylogenetic and functional distances are inversely related, and thus, we call the resulting diversity metrics decoupled.

In contrast, if species in a community have dissimilar traits, the community has a high phenotypic variation, which is equivalent to a high FD. High FD can either happen in combination with high phylogenetic variation (*Fig. 1*, top right) or phylogenetic clustering (*Fig. 1*, top left). Again, in the former case phylogenetic and functional diversities are coupled, while being inversely related, and therefore decoupled, in the latter case[21,22]. Many local studies found a prevalence of coupled communities with positive covariation of functional and phylogenetic diversity (FD, PD, respectively)[23–25], but negative covariations[26,27] and unclear patterns[28] have also been encountered. However, it is not yet known under which conditions communities express coupled or decoupled functional and phylogenetic diversities.

By calculating functional and phylogenetic diversity for 1,781,836 vegetation plots from sPlot[29], the global vegetation plot database, we tested whether patterns of coupling or decoupling 1) dominate at the global level, 2) show regional patterns, 3) differ between forest and non-forest ecosystems, and 4) correlate with recent and past climatic gradients. We hypothesized an overall coupled pattern of functional and phylogenetic diversity, since phylogenetic diversity has often been found to reflect functional trait diversity, especially for those phylogenetically conserved traits which are not easily measurable in plants, such as herbivore and pathogen resistance[15,20,30]. We expected higher phylogenetic diversity in forests than in non-forest ecosystems due to the co-occurrence of woody and non-woody plant species, given that the herbaceous habit has evolved from the ancestral woody state multiple times and in different lineages[31–34]. Since phylogenetic and functional diversity metrics are correlated with species richness, we used null models to calculate standardized effect sizes and quantify how much phylogenetic and functional diversity differed from random expectations before comparing them[35].

Results

The relationship of functional and phylogenetic diversity

We modelled the relationship between functional and phylogenetic diversity indices expressed as a standardized effect size of Rao´s quadratic entropy based on functional traits ($SES.FD_Q$) and phylogenetic distances ($SES.PD_Q$). We considered three functional traits representing the main dimensions of the global spectrum of plant form and function, namely the leaf economics spectrum (specific leaf area), the size-seed mass dimension (plant height), and the root collaboration gradient (specific root length)[36,37]. Both diversity indices were calculated as standardized effect sizes, based on biome-specific null models that account for the varying species richness across plots, and use the relative frequencies of species occurrences within each biome to weight species resampling probabilities. This was done because both functional and phylogenetic diversity are tightly related to species richness. Out of 1,781,836 vegetation plots, 31.38% showed trait and phylogenetic coupling as $SES.FD_Q$ and $SES.PD_Q$ were simultaneously high or low; 53.03% of the vegetation plots had higher $SES.FD_Q$ than $SES.PD_Q$ and 15.6% had higher $SES.PD_Q$ than $SES.FD_Q$, suggesting that decoupled plant communities are twice as common than coupled ones and that, on average, global communities are more functionally than phylogenetically diverse (*Fig. 2 A*). These results did not change after removing non-significant standardized effect values, i.e., values between -1.96 and 1.96 standard deviations from the mean (6.9% coupled communities, 45.8% decoupled with high FD values and 17.3% decoupled with high PD values).

We did not find any clear geographical pattern at the global scale (*Fig. 2 B*). Decoupled communities with high $SES.FD_Q$ and low $SES.PD_Q$, (see Methods for definition of high and low values of $SES.FD_Q$ and $SES.PD_Q$) occurred in the western USA and locally across Europe, while communities with low $SES.FD_Q$ and high $SES.PD_Q$ were found close to the Arctic Circle in Scandinavia and Siberia, and in New Zealand and Japan. Coupled communities with high values of both diversity indices were encountered in the eastern USA, Central-Europe as well as in New-Zealand and Japan.

Overall, we found a negative relationship between $SES.FD_Q$ and $SES.PD_Q$. Accounting for the spatial structure of the data by adding a smoothing spline, our general additive model explained 7.8% of the deviance in $SES.FD_Q$ (*Fig. 2 A*). Modelling the raw values of FD_Q against the raw values of PD_Q, hence not accounting for the effect of species richness, also returned a negative relationship with 18.5% of deviance explained (*Fig. S 1 A*). The explained deviance increased to 36.2% when the distance matrix of phylogenetic distances was square root-transformed, accounting for the non-linearity of trait evolution (*Fig. S 1 B*).

The negative relationship between $SES.FD_Q$ and $SES.PD_Q$ was robust to the use of alternative null models, diversity indices, selections of functional traits, and subsets of vegetation plot data (see Methods for details). Using a null model based on a global species pool, $SES.PD_Q$ together with the spatial smoothing spline explained 5.8% of the deviance in $SES.FD_Q$, which increased to 6.2% when the phylogenetic distances were square root-transformed (*Fig. S 1 C, D*). Based on a biome-specific, but unweighted species pool, the explained deviance was 6.8% (*Fig. S 1 F*). When null models were constrained based on a phytogeographic[38] species pool the explained deviance was 7.8% (*Fig. S 1 G*). The same negative relationship was found when using alternative indices of functional and phylogenetic diversity, i.e., when modelling standardized effect size of functional dispersion against mean pairwise distance (MPD). The explained deviance in this case was 7.1% (*Fig. S 1 E*). Considering each trait individually, or including additional traits (eight, see Methods for details) but only for an environmentally-balanced subset of vegetation plot data (i.e., sPlotOpen[39]), also returned a negative relationships between FD_Q and PD_Q (*Fig. S 7*, *Table S 1*).

The environmental predictors

We used Boosted Regression Trees (BRT) to select the environmental variables that best explain either $SES.FD_Q$ or $SES.PD_Q$. The BRTs suggested climatic variables to be most relevant for shaping patterns of $SES.FD_Q$ (*Fig. 3 A*). Temperature of the coldest quarter and coldest month (both reflected by PC2 in a principal component analysis based on 19 bioclimatic variables) had the highest relative influence on $SES.FD_Q$, followed by the climatic variability after the Last Glacial Maximum (LGM) and precipitation seasonality (PC5). Partial dependence plots suggested a predominantly positive relationship between $SES.FD_Q$ and climatic variability after the LGM and a negative one with precipitation seasonality (PC5, *Fig. S 3*). $SES.FD_Q$ first increased and then decreased with increasing temperatures of the coldest quarter and coldest month (PC2).

Regarding phylogenetic diversity, $SES.PD_Q$ was especially related to the vegetation formation type (forest vs. non-forest, classified based on the cover of the tree layer and species traits, such as growth form and height, see Methods), being higher in forest compared to non-forest ecosystems, and tended to increase with annual precipitation (PC1; *Fig. 3 A, Fig. S 4 A*).

When modelling the log ratio of $SES.FD_Q$ to $SES.PD_Q$, BRTs showed that the classification of forest / non-forest and annual precipitation (PC1) had the highest relative influence, resembling what we observed for $SES.PD_Q$ (*Fig. 3 B, S 4 B*).

From the BRTs, we chose variables with a relative influence greater than 12.5% (the relative influence expected by chance given by 100% / 8 explanatory variables) to use in general additive models (GAM) predicting $SES.FD_Q$ or $SES.PD_Q$ after accounting for spatial autocorrelation. The model for $SES.FD_Q$ explained 4.6% of the deviance and suggested that functional diversity increases with increased climatic variability after the last glacial maximum and temperatures of the coldest quarter or month (PC2, *Fig. 4*) and decreases with precipitation seasonality (PC5).

In contrast, the model for phylogenetic diversity showed higher explanatory power (37.3% of the deviance) with annual precipitation (PC1), vegetation type, and the spatial spline all affecting $SES.PD_Q$. Forests and sites with increased precipitation had higher $SES.PD_Q$ (*Fig. 5*). Modeling the log ratio between $SES.FD_Q$ and $SES.PD_Q$ confirmed that effects of $SES.PD_Q$ dominate, accounting for 30.8% of the deviance (*Fig. 6*).

To explore effects of environmental predictors on overall patterns of coupling and decoupling, we modelled the relationship between $SES.FD_Q$ and $SES.PD_Q$ as an ordered categorical variable with three states. This acknowledges that while there is only one way for communities to be coupled, decoupling can occur with either PD > FD, or FD > PD. Doing this resulted in a model that explained 10.2% of the deviance (*Fig. S 5*). Annual precipitation (PC1), precipitation seasonality (PC5), and forest / non-forest had the most power to discriminate the three categories.

Discussion

Plant communities differ in their functional and phylogenetic composition. Here, we modelled relationships between functional and phylogenetic diversity in plant communities across the globe to infer which factors best predict these separate facets of diversity. Values of functional and phylogenetic diversity tend to be decoupled, suggesting global patterns of community assembly are primarily driven by either functional or phylogenetic diversity rather than the two being integrated. Recent climatic conditions and past climatic conditions tended to drive differences in functional diversity (FD). As predicted, we found higher phylogenetic diversity (PD) in forest vs. non-forest communities. The log ratio of FD and PD varied with vegetation type (forest vs. non-forest) and recent climatic conditions, in line with what we observed for PD.

Contrary to our hypothesis, we found a negative but weak relationship between FD and PD at the global scale (*Fig. 2 A*). As PD is often considered to be a proxy for capturing unmeasured patterns of species functional traits, we expected a positive relationship between FD and PD[40], as postulated also by theoretical studies[25]. The negative correlation observed at the global scale shows that functional and phylogenetic diversity are more often decoupled than coupled in plant communities, with communities either having high phylogenetic or functional diversity, which is in line with recent results in grassland communities[26]. Additionally, distribution of traits across phylogenies can vary at small spatial scales, leading to both trait clustering and overdispersion[15,20]. This indicates that, contrary to the expected coupling of FD and PD, closely related species often exhibit considerable differences in trait values, while phylogenetically distant species can often share similar trait values. It is possible that co-occurring species with similar traits differ in other, not easily measurable traits, e.g., herbivory resistance, which are captured by phylogeny but less so by other functional traits. Functional clustering could reflect equalizing competitive dynamics in neutrally assembled communities[41] or broader-scale environmental filters. Additionally, when considering lineages' biogeographic histories, phylogenetic clustering could arise due to recent stochastic extinctions or limited dispersal following allopatric speciation[42].

The observed negative covariation between PD and FD might also be explained by the different impacts of biotic interactions and environmental filtering across communities[41,43,44].

In phylogenetically clustered communities, competitive exclusion may act as a primary mechanism, favoring the co-existence of species with dissimilar phenotypes and thus higher FD. In contrast, environmental filtering seems to be the driving process in communities with low FD and high PD. Here, only species with specific phenotypes are admitted to the community[45], but if these come from different clades, the community will exhibit functional convergence but phylogenetic variation. This pattern also suggests that species can differ in features not captured by the traits we use to calculate FD[46]. Since most communities show decoupling with high FD (53%), competition may drive global plant community assembly processes most strongly. However, we must consider that trait divergence can also arise from environmental factors that are spatially nested and interact with each other in filtering species within a community. That is, trait divergence is generated within the studied community units when the filtering effects of fine-scale environmental factors, such as those related to soil and herbivory, interact with and are nested within coarse-scale factors, such as climate[14]. In communities with intermediate values of PD, environmental filtering and competitive exclusion appear to be equally important, resulting in coupled communities. However, the relative importance of these mechanisms is difficult to test as we do not know whether species are excluded from any given community due to the environmental conditions, biotic interactions, dispersal limitation, or interactions among multiple factors[14,47]. FD and PD could then be decoupled in communities where geographical and local drivers differentially combine with biotic interactions to affect species' functional and phylogenetic relationships.

We observed no clear spatial patterns relating functional to phylogenetic diversity. Plots with coupled and decoupled FD and PD often occurred in geographical proximity, suggesting that local factors can dominate community assembly within regions (*Fig 2 B*). Previous studies reported geographical patterns of functional diversity based on climatic conditions, such as precipitation gradients[48]. Similarly, phylogenetic diversity tends to decrease polewards[49,50]. Studies on the global distribution of PD showed striking differences across ecoregions or biomes[51,52]. Such regional diversity patterns rarely translate into global patterns as broad-scale environmental conditions rarely correspond to local ecological conditions. Nevertheless, treating relationships between functional and phylogenetic diversity as a three-level categorical variable ("Decoupling with higher PD", "Coupling", "Decoupling with higher FD") allowed us to demonstrate that coarse-scale environmental factors do play a role (*Fig. S 5*). This suggests that even though we could not explain the full range of possible combinations of FD and PD, broader biogeographical patterns emerge.

Although SES.FD$_Q$ and environmental conditions sometimes covary, we failed to show that SES.FD$_Q$ is strongly driven by those conditions at the global scale (*Fig. 4*). In particular, functional diversity was not well explained by recent climatic conditions and climatic variability after the Last Glacial Maximum (LGM). This is in line with studies suggesting that the functional composition of local communities depends mostly on local factors, such as land-use history, soil properties, and microclimatic conditions[24,53]. However, a fine classification of biomes as functional units or vegetation types, as was done in a recent Europe-wide analysis on climate-trait relationship[54] might increase the explanatory power of our model.

Phylogenetic diversity (SES.PD$_Q$) was consistently higher in forests compared to non-forest ecosystems, suggesting that different layers within forest communities support diverse evolutionary histories (*Fig. 5*). Most tree species belong to predominantly woody families, many of which are phylogenetically distant from other plant families, augmenting the phylogenetic diversity found in forest ecosystems[31–33]. This is particularly true for forest conifers which represent a clade of woody species that separated from today’s angiosperms as early as 300 Mya[19]. Many forest understories also support cryptogams (including vascular ferns and lycopods) with distinct evolutionary histories relative to trees, further increasing phylogenetic diversity in forests[55,56]. These taxa also occur as epiphytes in tropical forests, contributing to their increased phylogenetic diversity. Stable microclimatic conditions under a closed canopy could also create conditions favoring species from distinct families[57,58]. Although stratification appeared to increase phylogenetic diversity, it did not increase functional diversity.

Overall, our findings suggest that while forest ecosystems display high phylogenetic diversity, the functional diversity of plant species in forests may be limited by convergence in functional traits across different layers. These analyses represent the first attempt to understand global relationships between functional and phylogenetic diversity but come with limitations. Although sPlot represents a global harmonized database of vegetation plots, its coverage is uneven across biomes and vegetation types, potentially biasing our results. We attempted to correct for this by down-sampled data from the temperate zone in favour of data from the tropics to an environmentally balanced subset. However, we observed an even stronger negative relationship between FD and PD. This suggests that tropical plant communities contribute disproportionately to this pattern. In addition, data in sPlot were collected using various sampling protocols and approaches, sometimes including only woody species and using plots of different shapes and sizes. We sought to partially overcome this problem by including predictors related to plot record characteristics (see Methods) and by calculating standardized effect sizes. Still, we do not know how these biases may have affected correlations between FD and PD. We also lacked information on the successional status of the vegetation plots, potentially influencing our results if early successional stages are lower in FD and PD compared to later successional communities. Because species abundance data are not well standardized in sPlot, it was more robust to use presence-absence data, but this might limit comparisons with other studies. It is also possible that the functional traits we selected might affect the relationships between functional and phylogenetic diversity we observed, especially given that we used only three traits to calculate FD. We note, however, that our results were robust to which traits were selected, individually or jointly, for calculating FD, with these not affecting the relationship between FD and PD (*Fig. S 7, Tab. S 1*).

Polytomies included in constructing the phylogeny might have led us to underestimate PD[59], which is why we used standardized effect sizes for PD. Additionally, we found the same negative pattern when we considered functional dispersion and mean pairwise distance (*Fig. S 1 E)* as proxy for FD and PD, where the latter is known to show different dispersion patterns than PD_Q[60]. However, when including PD as an explanatory variable in future studies, it is important to consider the relationship between traits and phylogeny and the potential non-linearity of trait evolution. Additionally, our analysis revealed that none of the potential traits exhibited a strong phylogenetic signal in all families considered in this study (*Fig. S 7 B*). Moreover, it appeared that certain families tend to possess more conserved traits compared to others. This is in line with other findings that evolutionary conservation can be associated with specific traits and lineages[38], but this is not a common pattern. Consequently, depending on the sampled community and plant species, different patterns may emerge in the relationship between FD and PD. While both plant characteristics and evolutionary history play crucial roles in community assembly processes, just which interacting mechanisms operate on which underlying biotic and abiotic factors remain unclear.

Our findings on the relationship of SES.FD$_Q$ and SES.PD$_Q$, imply that ecological communities can exhibit many combinations of functional and phylogenetic diversity. The decoupling of FD and PD found here plus the overall slightly negative correlation imply that competitive exclusion may commonly occur in plant communities. Our results also highlight the need to conserve both functional and phylogenetic diversity if we are to safeguard biodiversity. Both FD and PD play key roles in community assembly and likely affect how species and their interactions within communities will respond to changing climates and other drivers of global change. Future research may reveal which regional conditions contribute to hotspots of FD and PD and why. Understanding the diverse and context-dependent nature of FD and PD will shed light on the complex dynamics of ecological communities and help us design schemes to better protect the diversity they support.

Methods

Species community data

The vegetation plot database sPlot[29] (www.idiv.de/splot) is a harmonized collection of national- and regional-scale vegetation-plot datasets. sPlot provides geo-referenced information on the presence and abundance of all vascular plants co-occurring in a sampling area, i.e., vegetation plot. The database version sPlot 3.0 holds a total number of 1,977,637 vegetation plot records from 160 datasets collected between 1873 and 2019, across six continents and most biomes, including 76,912 vascular plant species (for version 2.1, see ref. 29). The size of a plot varies according to the type of vegetation being sampled; from 1 m^2 in grasslands to 250,000 m^2 in forest ecosystems. The vegetation type of a plot was classified as forest and non-forest based on tree layer cover and the growth form of dominant species[29]. Vegetation plot records were included in the study if the cumulative coverage of species for which both trait and phylogenetic information was available accounted for at least 50% of the relative vegetation cover in that plot (see below).

In addition, we used sPlotOpen[39], which is an environmentally balanced, open-access subset of sPlot, as a benchmark of our results, both when testing for the effect of trait selection when calculating functional diversity, and for the effect of uneven coverage of sPlot data across the Earth`s biomes.

Functional diversity

Plant functional traits were available from the gap-filled version of the TRY 5.0 database[61–64]. We calculated functional diversity as Rao’s quadratic entropy (FD_Q) as well as functional dispersion (FDis) for all vegetation plots in sPlot 3.0. The calculation of Rao’s quadratic entropy[65] is based on a Gower distance matrix calculated for the species present in each vegetation plot. FDis was computed from the uncorrected species-species distance matrix with the function *dbFD* from the R-package *FD*[66,67]. We based this calculation on three functional traits selected to cover most of the variation within plant traits and to represent different axes in the plant economic spectrum, i.e., belowground and resource strategy of acquisition or conservation (specific root length, specific leaf area) and reproduction strategy of quality or quantity (plant height)[37,68]. To evaluate the influence of trait selection on the relationship of functional and phylogenetic diversity, we calculated FD_Q on eight functional traits (specific leaf area, specific root length, seed mass, plant height, leaf phosphorus and nitrogen content, leaf dry matter content, chromosome number), both taken individually and jointly. We did this additional analysis based on the sPlotOpen subset only, since calculating standardized effect sizes (see below) of FD calculated on eight traits in all plots was computationally unfeasible, even using a High-Performance Cluster. Additionally, considering all eight traits for the complete dataset would have led to a loss of approximately 2000 species (~10% of species considered in this study, see below) due to missing data in the TRY database.

Functional traits can be conserved in the phylogeny. This was tested with two evolutionary models, i.e., Blomberg`s *K* and Pagel`s *λ*, where the latter is known to be more robust against incomplete resolved phylogenies or suboptimal branch lengths[17,18]. Blomberg`s *K* and Pagel`s *λ* were calculated using the function *phylosig* from the R-package *picante*[69]*.* In contrast to other tests for phylogenetic signals both models can be used to compare phylogenetic signals across different phylogenies[17], which needs to be done as a global plant phylogeny is simply too large for an appropriate calculation of phylogenetic signals. Therefore, the phylogenetic signal for each trait was calculated within each family. All eight functional traits showed either no or low phylogenetic signals for Pagel`s Λ and Blomberg`s *K* (*Fig. S 7 B & C*). Therefore, we assume that there is also no phylogenetic signal across vascular plants for the considered traits.

Phylogenetic diversity

For all species present in sPlot, a phylogenetic tree was built using the function *phylo.maker* from the R-package *V.PhyloMaker*[70]. The phylogenetic backbone of the package is the combination of GenBank taxa with a backbone provided by the Open Tree of Life, version 9.1 (GBOTB), for seed plants[71] and the clade of pteridophytes[72]. Missing genera were inserted to the half point of the family tree. This approach was evaluated by ref. 73, who showed that phylogenetic indices based on the calculated tree were highly correlated with indices based on the “PhytoPhylo megaphylogeny” (updated phylogenetic tree from ref. 72). Species that could not be inserted by the *phylo.maker* were bound to the half of the terminal level of a sister species if only one species was available in this genus, or to the most recent ancestor

(MRCA) if the genus included more than one species. This additional binding was done with the *bind.node* function from the R-package *phytools*[74].

The computed phylogenetic tree for sPlot contained 160 families with 68,052 of 76,912 species (88%) present within the database. Additional 3,802 species were included, with 3,348 being bound to the node of the most recent ancestor (MRCA) of already present sister species and 454 species to the half of the terminal level on the family node. The final phylogenetic tree contained 71,854 species on 32,395 nodes. A total of 31,727 species in the phylogeny also had traits in the TRY database. Of this subset, 322 species (approx. 1%) were bound to the half of the terminal level on the family node and 2766 (approx. 9%) to the MRCA. Vegetation plot records were only included in the analysis if both trait and phylogenetic information was available for at least 50% of the total relative cover of the species in that plot. In total, 1,781,836 out of 1,977,637 plot records remained.

Phylogenetic diversity was calculated as Rao`s quadratic entropy (PD_Q) which amounts to the mean nearest taxon distance for presence-absence data. We used the function *raoD* from the R-package *picante*[69], which is based on the cophenetic distance of all *n* species in the phylogeny, pruned to contain only the species in that plot. To account for the non-linearity of evolutionary histories, we also calculated PD_Q based on the square root-transformed cophenetic distance[75]. Additionally we calculated mean pairwise distance (MPD), to be compared with functional dispersion, as MPD could show opposite dispersion patterns than PD_Q[60]. Only species with both trait information and known phylogeny were used to calculate functional and phylogenetic diversity.

Standardized effect size

The species richness of the vegetation plot records ranged from one to 412 species (*Fig. S 8*). Functional and phylogenetic diversity indices are known to depend on species richness[76–78]. Especially for functional diversity, a higher number of species in a community is more likely to return higher functional diversity values than communities with fewer species[77]. We controlled for species richness by calculating the standardized effect size of each diversity index for every vegetation plot record[79], fixing the number of species of the plot record and drawing species randomly, which is equivalent to shuffling traits across species. As species do not equally occur across the globe, we calculated our null expectations based on biome-specific species pools accounting for the frequency of species in the plot records in each biome. However, to see if the patterns also hold true for broader species pools we used the following hierarchical approach with four stages of defined species pools. For the simplest species pool, we calculated our null expectations based on all species present in the whole sPlot database, so we allowed each species to occur everywhere in the world. For a more geographically constrained approach we calculated the null expectations based on species pools within 16 phytogeographical units[38] (stage 2) and ten predefined biomes (stage 3) in response to global climate variation[29,80], namely: alpine, boreal zone, dry mid-latitudes, dry tropics and subtropics, polar and subpolar zone, subtropics with winter rain, subtropics with year-round rain, temperate mid-latitudes, tropics with summer rain, and tropics with year-round rain. The fourth and most complex null model was based on the species pool within each biome, additionally sampling the species weighted by their frequency in the plot records within each biome. This means a species that occurred more frequently within a biome was randomly drawn more often to recalculate the null diversity index, compared to a species occurring less often. For each of the four null models, we calculated the mean and standard deviation of the distribution of null functional and phylogenetic indices across 499 draws. Vegetation plots only containing one species or for which trait and phylogenetic information was not available were excluded from functional or phylogenetic diversity calculations. Standardized effect sizes (SES) were obtained by subtracting the mean index of the randomized data from the observed index and dividing the result by the standard deviation of the index of the randomized data.

Definition of coupling and decoupling

To measure the percentage of coupled and decoupled communities a confidence interval was defined. We randomly drew one million values from a uniform distribution, defined between the minimum and maximum of observed standardized effect sizes of Rao´s quadratic entropy based on functional traits ($SES.FD_Q$) as explanatory variable. We created a correlated response variable by adding an error from a normal distribution, obtained from the mean and the standard deviation of the observed $SES.FD_Q$. We fitted a linear model and extracted the intercept and the confidence interval. Communities with an observed value of $SES.FD_Q$ were considered coupled if the standardized effect sizes of Rao´s quadratic entropy based on phylogenetic distance ($SES.PD_Q$) fell within this interval. Based on this, we defined three categories of community patterns, i.e., “Decoupling with higher FD than PD”, “Coupling” and “Decoupling with lower FD than PD”. This variable was later used as an ordered categorical response. Additionally, we calculated the log ratio between $SES.FD_Q$ and $SES.PD_Q$ as $\log(SES.FD_Q/SES.PD_Q)$ after scaling the values between 0.001 and 1. Positive and negative values define the deviation with higher and lower $SES.FD_Q$ than $SES.PD_Q$, respectively, from a perfect coupled community.

Explanatory variables

Recent climatic conditions (1981-2010) were represented by the 19 bioclimatic variables from CHELSA v.2.1[81,82]. A principal component analysis (PCA) was performed to reduce data dimensionality. In the following analyses, we only used the first five PCA axes, collectively accounting for 92.3% of the explained variation. We interpreted the axes based on the highest loadings of the corresponding climatic variable as follows: annual precipitation for PC1; mean daily air temperature of the coldest quarter and mean daily minimum air temperature of the coldest month for PC2; annual air temperature range for PC3; isothermality for PC4; and precipitation seasonality for PC5 (*Tab. S 2*, *Fig. S 9*).

Mean air temperature variability after the Last Glacial Maximum (LGM) was derived from the open-access StableClim v1.1. dataset, containing estimates from 21,000 years ago at 2.5° spatial resolution[83]. Climatic variability represents rapid global warming during the last deglaciation during the Bølling-Allerød transition[84] on land and sea. The mean temperature variability between 21,000 B.P. and 100 A.D. was used as index for the climatic variability after the LGM.

All climatic variables were extracted for each plot with the *extract* function from the R-package *raster*[85].

Not all vegetation plot records were complete in terms of the sampled functional groups. Records from tropical forest plots often contained either only tree data, or tree and shrub data. As the exclusion of those plots would have substantially reduced the spatial coverage of our model, we added the nominal predictor variable called ‘plants recorded’ to our models to partially control for this source of bias. The variable ‘plants recorded’ has four values: all vascular plants, only dominant species, all woody plants, only trees. Additionally, we used the vegetation type (forest vs. non-forest) from the vegetation plot database sPlot as predictor variable.

In total, we prepared eight explanatory variables, five related to the recent climatic conditions, one to past climatic variability, and two to plot record characteristics.

Statistical modelling

A generalized additive model (GAM) was used to model the relationship between functional and phylogenetic diversity, either expressed as observed Rao`s quadratic entropy (for phylogenetic diversity also after a square root transformation of the distance matrix), or as standardized effect size of Rao`s quadratic entropy, functional dispersion and mean pairwise distance. A GAM is a generalized linear model in which the linear response can depend on unknown smooth functions of the explanatory variables. To account for the spatial structure of the data, the spatial coordinates were included as smooth spherical splines. All GAMs included a basis penalty smoother spline on the sphere (bs = ”sos”), applied to the geographic coordinates of every plot, thus taking spatial autocorrelation into account. The explanatory variable was included as linear predictors without any smooth function. The model was performed using the function *gam* from the R-package *mgcv*[86–91], defined as following:

gam(SES.FD$_Q$ ~ SES.PD$_Q$ + s(Longitude, Latitude, bs = "sos"), family = "gaussian", method = "REML")

SES.FD$_Q$ is the standardized effect size of Rao's quadratic entropy based on the three selected functional plant traits and SES.PD$_Q$ is the standardized effect size of Rao's quadratic entropy based on the phylogenetic distances of species present in the community. This step was done for the complete dataset and for the sPlotOpen subset, for which we considered the eight traits, both individually and jointly, for calculating standardized effect size of FD.

To model the relationship between either functional or phylogenetic diversity and the set of the eight explanatory variables described above, we used a two-step approach. In the first step, we used Boosted Regression Trees (BRTs) to select relevant explanatory variables and quantify their relative influence. In the second step, we fitted GAMs using functional, phylogenetic diversity or their log ratio as response variables, and the predictors selected in the first step as explanatory variables. We did this because fitting a full GAM algorithm with all predictors would lead to convergence issues, due to the huge number of data points.

BRTs are a machine-learning technique used in regression and classification having few prior assumptions and being robust against overfitting and collinearity. They are known to uncover nonlinear relationships as well as interactions among predictors. The parameters of the BRT were set as follows: a tree complexity of five and a bag fraction of 0.5. The learning rate was set to 0.01 with a maximum number of 20,000 trees. The BRTs were calculated using the *gbm.step* routine from the *dismo* package[92]. An explanatory variable was considered relevant in the model if its relative influence was greater than 12.5%, which is the expected influence of a variable if all the eight predictors had an equal relative importance.

The variables that were considered as relevant from the BRTs were then used in a second set of GAMs, having as response variable either functional diversity ($SES.FD_Q$), phylogenetic diversity ($SES.PD_Q$) or their log ratio, and as explanatory variables those that turned out to be relevant in the corresponding BRT. Additionally, we fitted a GAM with the ordered categorical response of coupling and decoupling against the environmental predictors, which were selected by the BRTs for functional and phylogenetic diversity. As the three categories were not equally represented, we sampled 10,000 communities for each category and repeated the GAM 100 times, besides running the same model on the complete (unbalanced) dataset. The spatial coordinates were included as smooth spherical splines in all models as explained above. As not all vegetation plot entries in sPlot are classified as forest / non-forest the number of observations for the environmental models was 1,497,238. The prediction of each explanatory variable was performed using the *prediction* function from the R-package *marginaleffects*[93] by predicting the explanatory variable based on the sequence between the minimum and maximum of the variable in the original data and the GAM model. The plotted regressions were obtained by extracting the residuals from a GAM without the explanatory variable of interest.

For plotting, functional and phylogenetic variables were averaged for each grid cell with a size of 863.8 km^2. The spatial smoother within the GAM was plotted at the same resolution based on the following model (example based on $SES.FD_Q$):

```
gam (SES.FD_Q ~ 1 + s(Longitude, Latitude, bs = "sos"), family = "gaussian", method = "REML")
```

All analyses were performed in R 4.1.3[94].

Data availability

Source data are provided with this paper. All calculated biodiversity indices necessary to reproduce the results of this manuscript are available at: https://doi.org/10.25829/idiv.3574-mpmk21[95]

The vegetation-plot raw data for sPlotOpen is available at: https://www.idiv.de/de/splot/splotopen.html
The vegetation-plot raw data contained in the sPlot database are available upon request by submitting a project proposal to sPlot's Steering Committee. The proposals should follow the Governance and Data Property Rules of the sPlot Working Group available on the sPlot website (www.idiv.de/splot).

Code availability

All R scripts used for this study can be found in our GitHub repository at https://github.com/georghaehn/Haehn-et-al-2024-FD-PD-coupling.

Acknowledgements

The authors are thankful for the efforts of thousands of vegetation scientists sampling and digitalizing vegetation data and making them available in regional, national, or international databases. We appreciate the support of the German Research Foundation for funding sPlot as one of the iDiv research platforms (DFG FZT 118, 202548816). The scientific results have (in part) been computed at the High-Performance Computing (HPC) Cluster EVE, a joint effort of both the Helmholtz Centre for Environmental Research - UFZ (http://www.ufz.de/) and the German Centre for Integrative Biodiversity Research (iDiv) Halle-Jena-Leipzig (http://www.idiv-biodiversity.de/). We would like to thank the administration and support staff of EVE who keep the system running and support us with our scientific computing needs: Thomas Schnicke, Ben Langenberg, Guido Schramm, Toni Harzendorf, Tom Strempel and Lisa

Schurack from the UFZ, and Christian Krause from iDiv. We would like to thank iDiv’s Data & Code Unit for assistance with curation (done by Dr. Ludmilla Figueiredo) and archiving of the dataset. F.M.S. gratefully acknowledges financial support from the Rita Levi Montalcini (2019) program, funded by the Italian Ministry of University and Research (MUR). J.-C.S. considers this work a contribution to Center for Ecological Dynamics in a Novel Biosphere (ECONOVO), funded by Danish National Research Foundation (grant DNRF173) and his VILLUM Investigator project “Biodiversity Dynamics in a Changing World”, funded by VILLUM FONDEN (grant 16549). V.D.P. received support from Conselho Nacional de Desenvolvimento Científico e Tecnológico (CNPq, Brazil, grant 313315/2022-1). I.B. and J.A.C. were funded by the Basque Government (IT1487-22). A.D.B was supported by the Knut and Alice Wallenberg Foundation (WAF KAW 2019.0202) and the Swedish Foundation for Strategic Research (FFL21-0194). A.G.-de-M. has been supported by National Forestry and Wildlife Service (SERFOR) of Peru (AUT-IFL-2023-017) and Fundación Universitaria San Pablo-CEU, grants GNRI 2023 and GNRI 2024. A.Č, F.K. and U.Š. were supported by the Slovenian Research and Innovation Agency (P1-0236).

Author contributions

G.J.A.H, F.M.S. and H.B. conceived the idea. G.J.A.H. performed the analysis with substantial input from F.M.S, G.D. and H.B. G.J.A.H. drafted the first version of the manuscript with support by F.M.S, G.D., M.S. and H.B. E.A.-D., I.A., M.B., E.B., I.B., A.D.B., G.B., Z.B.-D., J.A.C., A.Č., M.C., R.Ć., A.L.G, M.D.S., Jü.D., J.D, M.E.-S., M.F., A.G.-d.-M., E.G., H.G., V.G., S.H., M.H., B.H., J.H., U.J., F.J., A.J., J.K., M.K., L.K., H.K., F.K., J.L., J.E.M., L.M., A.N., J.N., A.P.-H., O.P., V.D.P., G.R., E.R., B.Sa., M.Sch., U.S., S.S., F.S., U.Š., B.Sp., M.S., Z.S., B.St., J.-C.S., C.T., Z.T., A.C.V., C.V., D.W, De.W., H.-F.W., T.W., and G.Z. provided parts of the data. All co-authors edited the manuscript and provided suggestions on how to improve the analyses.

The authors declare no competing interests.

Figures

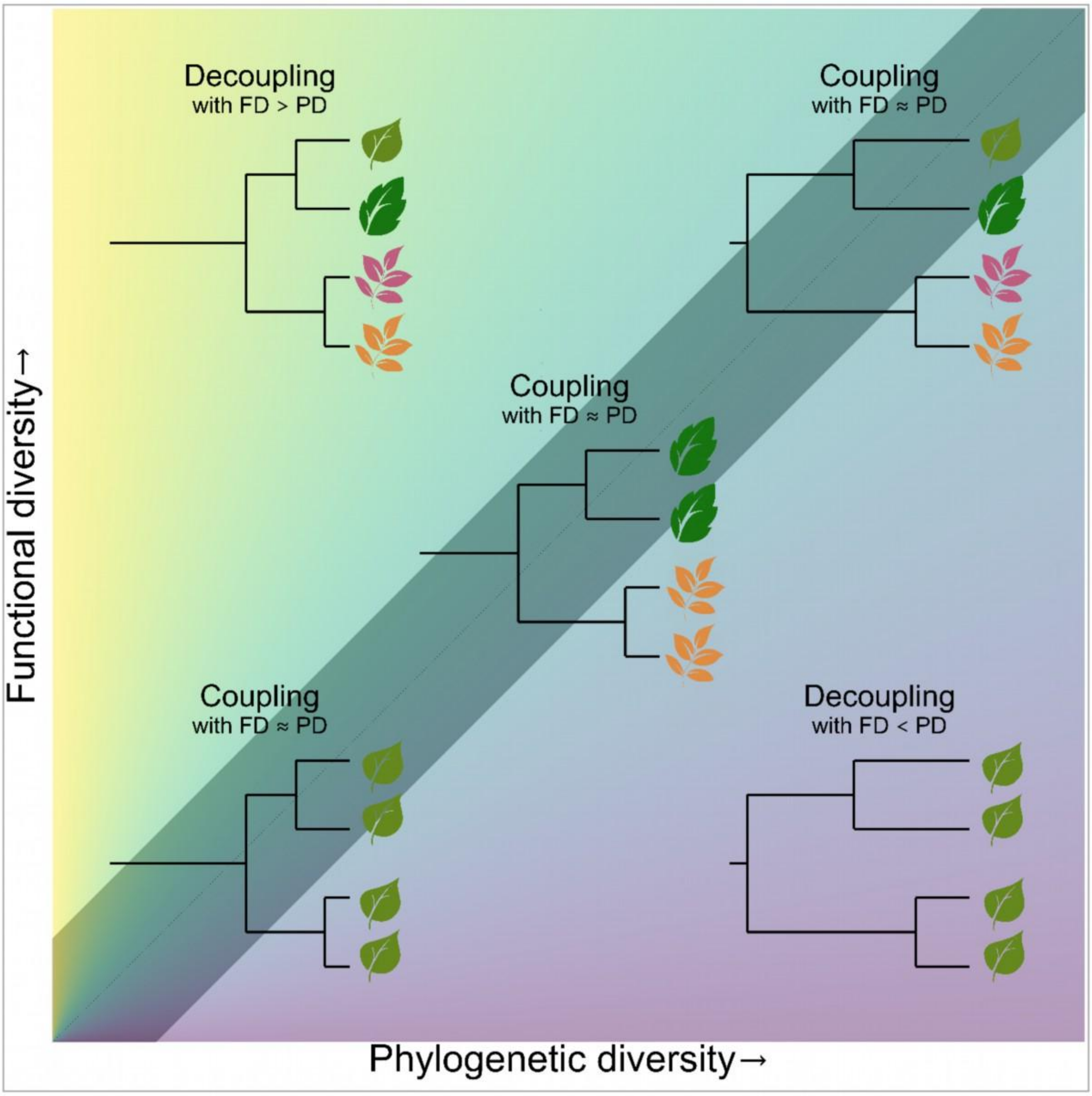

Figure 1: Conceptual figure of the relationship between functional and phylogenetic diversity after Ref. 20 & 21. If functional diversity is proportional to community phylogenetic diversity, we consider the community to be coupled (diagonal). The extremes are the results either of phylogenetic clustering in combination with trait convergence (bottom left) or phylogenetic overdispersion in combination with trait divergence (top right). Decoupled communities can be either observed if a community shows phylogenetic overdispersion in combination with trait convergence (bottom right) or if it shows phylogenetic clustering with trait divergence (top left).

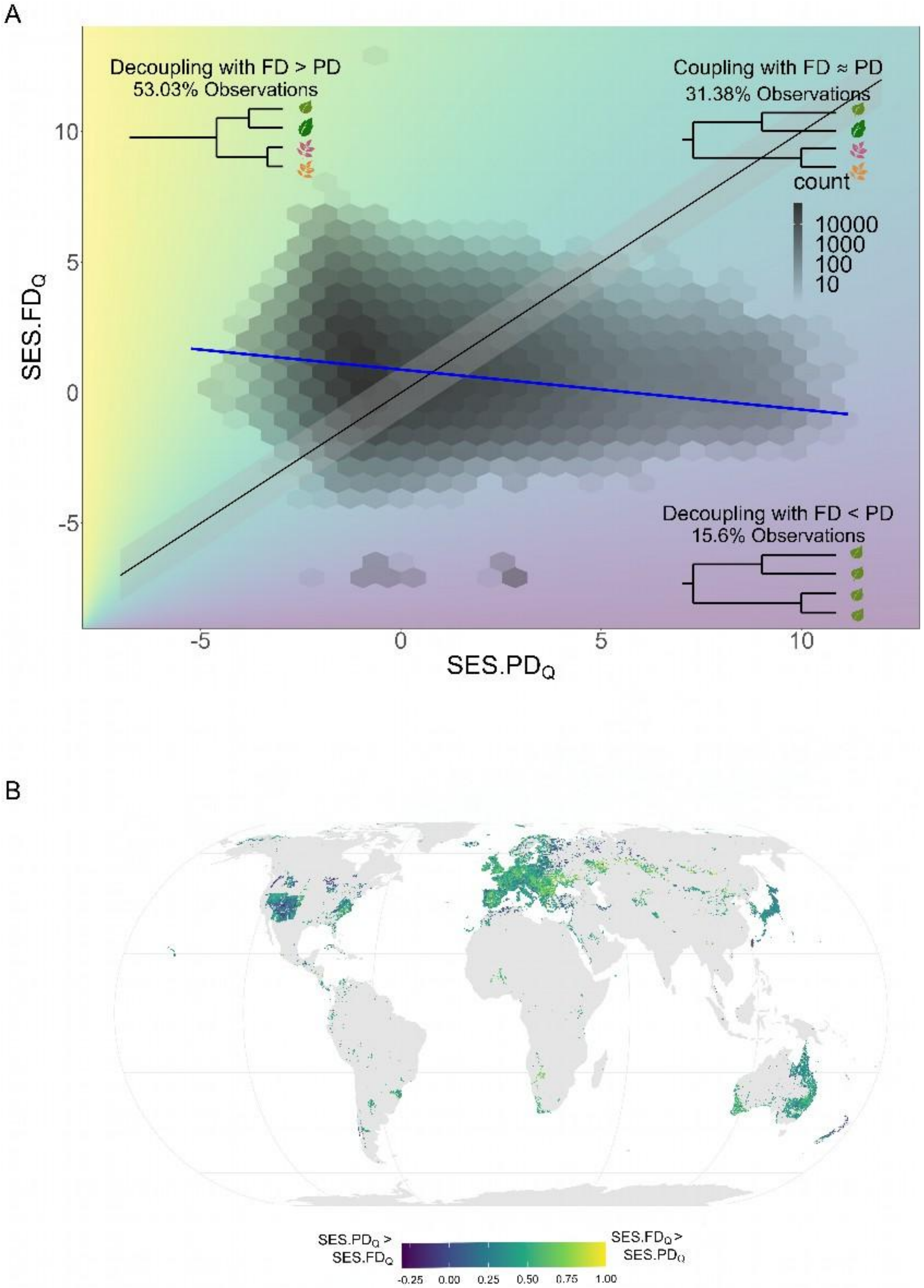

Figure 2: The relationship of standardized effect size of quadratic functional (SES.FD$_Q$) and phylogenetic diversity (SES.PD$_Q$). SES.FD$_Q$ is based on three functional traits: specific leaf area, plant height and specific root length. ***A*** *SES.FD$_Q$ as a function of SES.PD$_Q$ with the linear*

regression slope (blue) after accounting for spatial autocorrelation within a general additive model (7.8% explained deviance). Additionally, the line of coupling with the 1:1 relationship (black) and the confidence interval (gray, see Methods), with 31.38% of the observations lying within the confidence interval and 53.03% and 15.6% show decoupling, with either FD > PD or FD < PD, respectively. ***B*** *Mean log ratio of standardized effect sizes of functional (SES.FD$_Q$) and phylogenetic diversity (SES.PD$_Q$) per raster cell (863.8 km^2). Negative values indicate higher observed SES.PD$_Q$ than SES.FD$_Q$ and vice versa. The extracted values from the spatial smoothing spline from the general additive model can be found in Fig. S 2 D.*

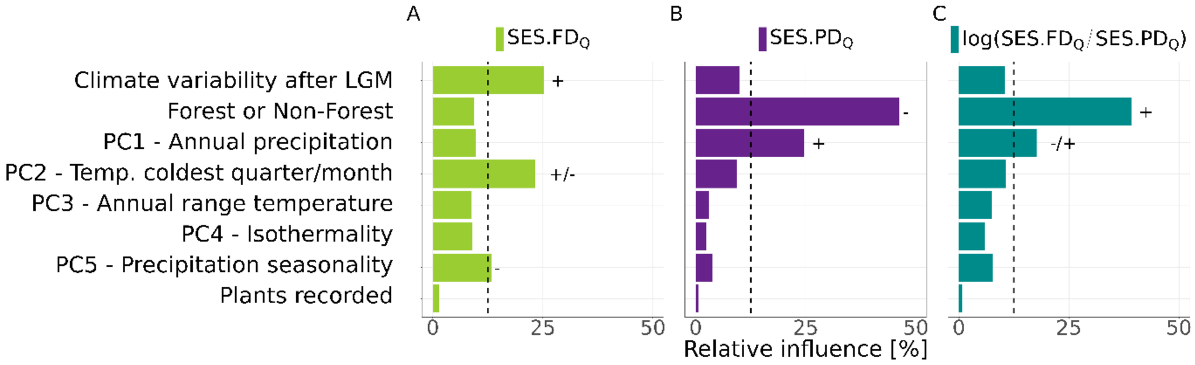

Figure 3: Results of the Boosted Regression Trees for ***A*** *SES.FD$_Q$,* ***B*** *SES.PD$_Q$ and* ***C*** *the logarithm of the ratio between SES.FD$_Q$ and SES.PD$_Q$. An explanatory variable was considered relevant in the model when its relative influence was greater than 12.5%, indicated by the dashed line, which is the expected influence of a variable if all eight predictors had the same relative importance. The signs indicate the direction of the significant effects based on the partial dependence models (Fig. S 3 & 4). Explanations of the abbreviations can be found under Fig. 2; LGM Refers to last Glacial Maximum.*

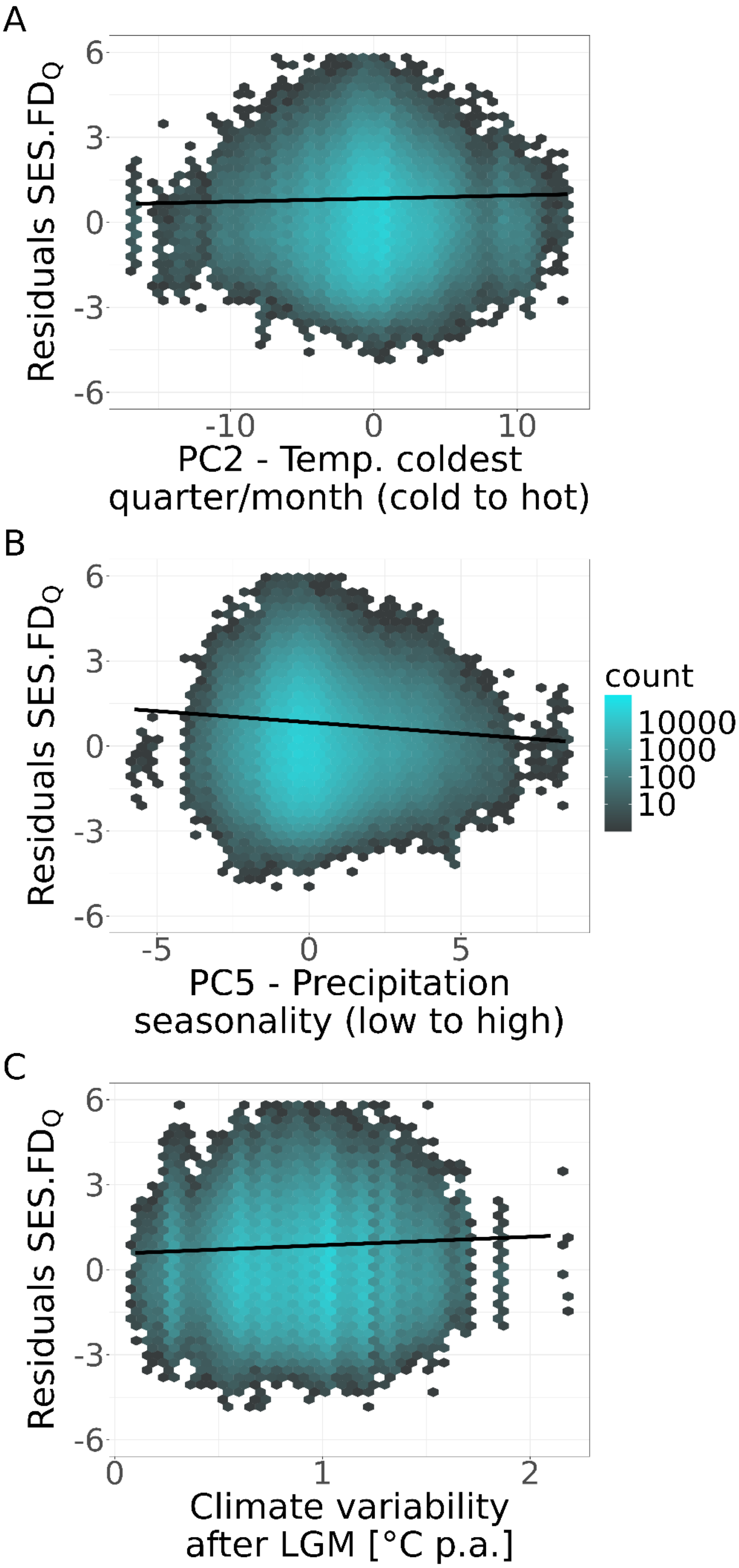

Figure 4: Predictors of

*the standardized effect size of functional diversity (SES.FD$_Q$). Residuals of SES.FD$_Q$ as a function of **A** temperature of the coldest quarter and month (PC2), **B** precipitation seasonality (PC5), and **C** climatic variability after the last glacial maximum. The generalized additive model (GAM) explained 4.6% of the deviance. The solid line shows the regression obtained from the GAM. The density hexagons show the distribution of the residuals of the model without the explanatory variable of interest. The smooth term of SES.FD$_Q$ can be found in Fig. S 6 A.*

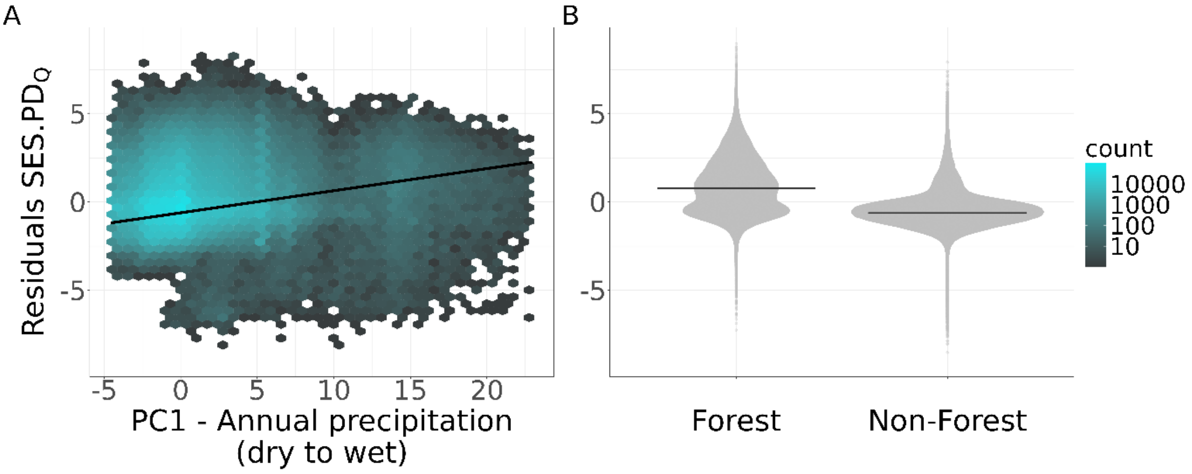

*Figure 5: Predictors of standardized effect size of phylogenetic diversity (SES.PD$_Q$). Residuals of SES.PD$_Q$ as a function of **A** annual precipitation (PC1), and **B** vegetation type. The generalized additive model (GAM) explained 37.3% of the deviance. The solid line shows the regression obtained from the GAM. The density hexagons show the distribution of the residuals of the model without the explanatory variable of interest. The smooth term of SES.PD$_Q$ can be found in Fig. S 6 B.*

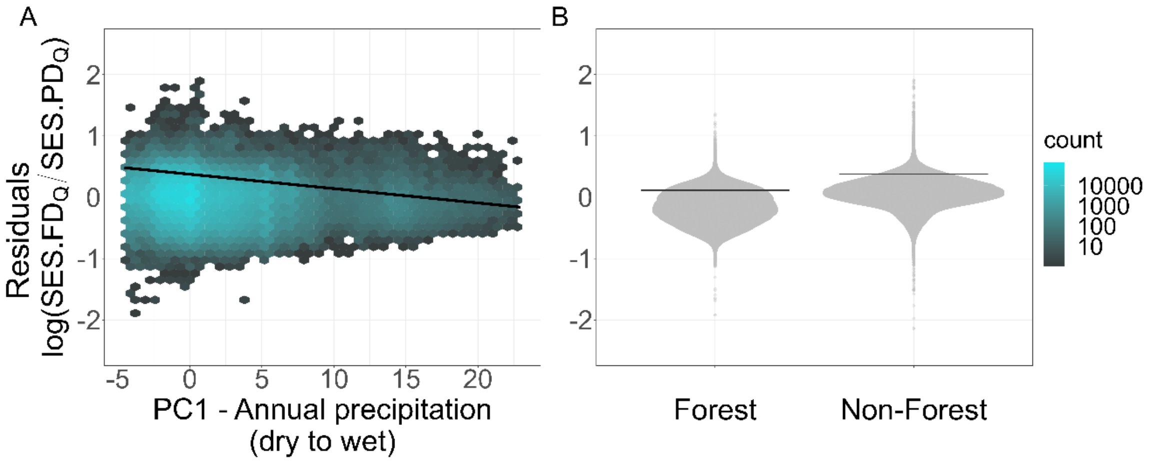

*Figure 6: Predictors of the log ratio between the standardized effect size of functional diversity (SES.FD$_Q$) and phylogenetic diversity (SES.PD$_Q$). Residuals of log(SES.FD$_Q$/SES.PD$_Q$) as a function of **A** annual precipitation (PC1), and **B** vegetation type. The generalized additive model (GAM) explained 30.8% of the deviance. The solid line shows the regression obtained from the GAM. The density hexagons show the distribution of the residuals of the model without the explanatory variable of interest. The smooth term of log(SES.FD$_Q$/SES.PD$_Q$) can be found in Fig. S 6 C.*

References

1. O’Connor, B., Bojinski, S., Röösli, C. & Schaepman, M. E. Monitoring global changes in biodiversity and climate essential as ecological crisis intensifies. *Ecological Informatics* **55**, (2020).

2. Anwar, M. R., Liu, D. L., Macadam, I. & Kelly, G. Adapting agriculture to climate change: a review. *Theoretical and Applied Climatology* **113**, 225–245 (2013).

3. Benevolenza, M. A. & DeRigne, L. The impact of climate change and natural disasters on vulnerable populations: A systematic review of literature. *Journal of Human Behavior in the Social Environment* **29**, 266–281 (2019).

4. IPCC, 2023: *Climate Change 2023: Synthesis Report.* Contribution of Working Groups I, II and III to the Sixth Assessment Report of the Intergovernmental Panel on Climate Change [Core Writing Team, H. Lee and J. Romero (eds.)]. IPCC, Geneva, Switzerland, 35-115 (2023)

5. Fahad, S. *et al. Climate Change and Plants: Biodiversity, Growth and Interactions*. (CRC Press, 2021).

6. Corlett, R. T. & Westcott, D. A. Will plant movements keep up with climate change? *Trends in Ecology & Evolution* **28**, 482–488 (2013).

7. Cavender-Bares, J., Kozak, K. H., Fine, P. V. A. & Kembel, S. W. The merging of community ecology and phylogenetic biology. *Ecology Letters* **12**, 693–715 (2009).

8. Götzenberger, L. *et al.* Ecological assembly rules in plant communities—approaches, patterns and prospects. *Biological Reviews* **87**, 111–127 (2012).

9. Rieseberg, L. H., Wood, T. E. & Baack, E. J. The nature of plant species. *Nature* **440**, 524–527 (2006).

10. Verdú, M. & Pausas, J. G. Fire drives phylogenetic clustering in Mediterranean Basin woody plant communities. *Journal of Ecology* **95**, 1316–1323 (2007).

11. Ackerly, D. D., Schwilk, D. W. & Webb, C. O. Niche Evolution and Adaptive Radiation: Testing the Order of Trait Divergence. *Ecology* **87**, 50–61 (2006).

12. Pillar, V. D., Duarte, L. da S., Sosinski, E. E. & Joner, F. Discriminating trait-convergence and trait-divergence assembly patterns in ecological community gradients. *Journal of Vegetation Science* **20**, 334–348 (2009).

13. Pillar, V. D., Sabatini, F. M., Jandt, U., Camiz, S. & Bruelheide, H. Revealing the functional traits linked to hidden environmental factors in community assembly. *Journal of Vegetation Science* **32**, e12976 (2021).

14. Pillar, V. D. Trait divergence in plant community assembly is generated by environmental factor interactions. *Journal of Vegetation Science* **35**, e13259 (2024).

15. Ackerly, D. Conservatism and diversification of plant functional traits: Evolutionary rates versus phylogenetic signal. *PNAS* **106**, 19699–19706 (2009).

16. Ávila-Lovera, E., Winter, K. & Goldsmith, G. R. Evidence for phylogenetic signal and correlated evolution in plant–water relation traits. *New Phytologist* **237**, 392–407 (2023).

17. Münkemüller, T. *et al.* How to measure and test phylogenetic signal. *Methods in Ecology and Evolution* **3**, 743–756 (2012).

18. Molina-Venegas, R. & Rodríguez, M. Á. Revisiting phylogenetic signal; strong or negligible impacts of polytomies and branch length information? *BMC Evolutionary Biology* **17**, (2017).

19. Melzer, R., Wang, Y.-Q. & Theißen, G. The naked and the dead: The ABCs of gymnosperm reproduction and the origin of the angiosperm flower. *Seminars in Cell & Developmental Biology* **21**, 118–128 (2010).

20. Cavender-Bares, J., Ackerly, D. D., Baum, D. A. & Bazzaz, F. A. Phylogenetic overdispersion in Floridian oak communities. *The American Naturalist* **163**, 823–843 (2004).

21. Cadotte, M., Albert, C. H. & Walker, S. C. The ecology of differences: assessing community assembly with trait and evolutionary distances. *Ecology Letters* **16**, 1234–1244 (2013).

22. Srivastava, D. S., Cadotte, M. W., MacDonald, A. A. M., Marushia, R. G. & Mirotchnick, N. Phylogenetic diversity and the functioning of ecosystems. *Ecology Letters* **15**, 637–648 (2012).

23. Webb, C. O. Exploring the Phylogenetic Structure of Ecological Communities: An Example for Rain Forest Trees. *The American Naturalist* **156**, 145–155 (2000).

24. Flynn, D. F. B., Mirotchnick, N., Jain, M., Palmer, M. I. & Naeem, S. Functional and phylogenetic diversity as predictors of biodiversity–ecosystem-function relationships. *Ecology* **92**, 1573–1581 (2011).

25. Tucker, C. M., Davies, T. J., Cadotte, M. W. & Pearse, W. D. On the relationship between phylogenetic diversity and trait diversity. *Ecology* **99**, 1473–1479 (2018).

26. Večeřa, M. *et al.* Decoupled phylogenetic and functional diversity in European grasslands. *Preslia* **95**, 413–445 (2023).

27. Prinzing, A. *et al.* Less lineages – more trait variation: phylogenetically clustered plant communities are functionally more diverse. *Ecology Letters* **11**, 809–819 (2008).

28. Kluge, J. & Kessler, M. Phylogenetic diversity, trait diversity and niches: species assembly of ferns along a tropical elevational gradient. *Journal of Biogeography* **38**, 394–405 (2011).

29. Bruelheide, H. *et al.* sPlot – A new tool for global vegetation analyses. *Journal of Vegetation Science* **30**, 161–186 (2019).

30. Castagneyrol, B., Jactel, H., Vacher, C., Brockerhoff, E. G. & Koricheva, J. Effects of plant phylogenetic diversity on herbivory depend on herbivore specialization. *Journal of Applied Ecology* **51**, 134–141 (2014).

31. Qian, H., Hao, Z. & Zhang, J. Phylogenetic structure and phylogenetic diversity of angiosperm assemblages in forests along an elevational gradient in Changbaishan, China. *Journal of Plant Ecology* **7**, 154–165 (2014).

32. Honorio Coronado, E. N. *et al.* Phylogenetic diversity of Amazonian tree communities. *Diversity and Distributions* **21**, 1295–1307 (2015).

33. Mastrogianni, A., Kallimanis, A. S., Chytrý, M. & Tsiripidis, I. Phylogenetic diversity patterns in forests of a putative refugial area in Greece: A community level analysis. *Forest Ecology and Management* **446**, 226–237 (2019).

34. Klimeš, A., Šímová, I., Zizka, A., Antonelli, A. & Herben, T. The ecological drivers of growth form evolution in flowering plants. *Journal of Ecology* **110**, 1525–1536 (2022).

35. Chai, Y. *et al.* Patterns of taxonomic, phylogenetic diversity during a long-term succession of forest on the Loess Plateau, China: insights into assembly process. *Scientific Reports* **6**, 27087 (2016).

36. Díaz, S. *et al.* The global spectrum of plant form and function. *Nature* **529**, 167–171 (2016).

37. Weigelt, A. *et al.* An integrated framework of plant form and function: the belowground perspective. *New Phytologist* **232**, 42–59 (2021).

38. Carta, A., Peruzzi, L. & Ramírez-Barahona, S. A global phylogenetic regionalization of vascular plants reveals a deep split between Gondwanan and Laurasian biotas. *New Phytologist* **233**, 1494–1504 (2022).

39. Sabatini, F. M. *et al.* sPlotOpen – An environmentally balanced, open-access, global dataset of vegetation plots. *Global Ecology and Biogeography* **30**, 1740–1764 (2021).

40. Reich, P. B. *et al.* The Evolution of Plant Functional Variation: Traits, Spectra, and Strategies. *International Journal of Plant Sciences* **164**, 143–164 (2003).

41. Mayfield, M. M. & Levine, J. M. Opposing effects of competitive exclusion on the phylogenetic structure of communities. *Ecology Letters* **13**, 1085–1093 (2010).

42. Pigot, A. L. & Etienne, R. S. A new dynamic null model for phylogenetic community structure. *Ecology Letters* **18**, 153–163 (2015).

43. Godoy, O., Kraft, N. J. B. & Levine, J. M. Phylogenetic relatedness and the determinants of competitive outcomes. *Ecology Letters* **17**, 836–844 (2014).

44. Kraft, N. J. B., Godoy, O. & Levine, J. M. Plant functional traits and the multidimensional nature of species coexistence. *Proceedings of the National Academy of Sciences* **112**, 797–802 (2015).

45. de Bello, F. *et al. Handbook of Trait-Based Ecology: From Theory to R Tools*. (Cambridge University Press, Cambridge, 2021).

46. Owen, N. R., Gumbs, R., Gray, C. L. & Faith, D. P. Global conservation of phylogenetic diversity captures more than just functional diversity. *Nature Communications* **10**, 859 (2019).

47. Kraft, N. J. B. *et al.* Community assembly, coexistence and the environmental filtering metaphor. *Functional Ecology* **29**, 592–599 (2015).

48. Zuo, X. *et al.* Functional diversity response to geographic and experimental precipitation gradients varies with plant community type. *Functional Ecology* **35**, 2119–2132 (2021).

49. Massante, J. C. *et al.* Contrasting latitudinal patterns in phylogenetic diversity between woody and herbaceous communities. *Scientific Reports* **9**, 6443 (2019).

50. Cai, H. *et al.* Geographical patterns in phylogenetic diversity of Chinese woody plants and its application for conservation planning. *Diversity and Distributions* **27**, 179–194 (2021).

51. Tietje, M. *et al.* Global hotspots of plant phylogenetic diversity. *New Phytologist* **240**, 1636–1646 (2023).

52. Qian, H., Zhang, J. & Jiang, M. Global patterns of taxonomic and phylogenetic diversity of flowering plants: Biodiversity hotspots and coldspots. *Plant Diversity* **45**, 265–271 (2023).

53. De Pauw, K. *et al.* Taxonomic, phylogenetic and functional diversity of understorey plants respond differently to environmental conditions in European forest edges. *Journal of Ecology* **109**, 2629–2648 (2021).

54. Kambach, S. *et al.* Climate-trait relationships exhibit strong habitat specificity in plant communities across Europe. *Nature Communications* **14**, 712 (2023).

55. Pryer, K. M. *et al.* Horsetails and ferns are a monophyletic group and the closest living relatives to seed plants. *Nature* **409**, 618–622 (2001).

56. Rothfels, C. J. *et al.* The evolutionary history of ferns inferred from 25 low-copy nuclear genes. *American Journal of Botany* **102**, 1089–1107 (2015).

57. De Frenne, P. *et al.* Forest microclimates and climate change: Importance, drivers and future research agenda. *Global Change Biology* **27**, 2279–2297 (2021).

58. Kovács, B., Tinya, F. & Ódor, P. Stand structural drivers of microclimate in mature temperate mixed forests. *Agricultural and Forest Meteorology* **234–235**, 11–21 (2017).

59. Swenson, N. Phylogenetic Resolution and Quantifying the Phylogenetic Diversity and Dispersion of Communities. *PloS ONE* **4**, e4390 (2009).

60. Sessa, E. B. *et al.* Community assembly of the ferns of Florida. *American Journal of Botany* **105**, 549–564 (2018).

61. Kattge, J. *et al.* TRY plant trait database – enhanced coverage and open access. *Global Change Biology* **26**, 119–188 (2020).

62. Shan, H. *et al.* Gap Filling in the Plant Kingdom: Trait Prediction Using Hierarchical Probabilistic Matrix Factorization. Preprint at https://doi.org/10.48550/arXiv.1206.6439 (2012).

63. Fazayeli, F., Banerjee, A., Kattge, J., Schrodt, F. & Reich, P. B. Uncertainty Quantified Matrix Completion Using Bayesian Hierarchical Matrix Factorization. in *2014 13th International Conference on Machine Learning and Applications* 312–317 (2014). doi:10.1109/ICMLA.2014.56.

64. Schrodt, F. *et al.* BHPMF – a hierarchical Bayesian approach to gap-filling and trait prediction for macroecology and functional biogeography. *Global Ecology and Biogeography* **24**, 1510–1521 (2015).

65. Rao, C. R. Diversity and dissimilarity coefficients: A unified approach. *Theoretical Population Biology* **21**, 24–43 (1982).

66. Laliberté, E. & Legendre, P. A distance-based framework for measuring functional diversity from multiple traits. *Ecology* **91**, 299–305 (2010).

67. Laliberté, E., Legendre, P. & Shipley, B. FD: Measuring functional diversity from multiple traits, and other tools for functional ecology. *R package version* **1**, 0–12 (2014).

68. Walker, A. P., McCormack, M. L., Messier, J., Myers-Smith, I. H. & Wullschleger, S. D. Trait covariance: the functional warp of plant diversity? *New Phytologist* **216**, 976–980 (2017).

69. Kembel, S. W. *et al.* picante: Integrating Phylogenies and Ecology. (2020).

70. Jin, Y. & Qian, H. V.PhyloMaker: an R package that can generate very large phylogenies for vascular plants. *Ecography* **42**, 1353–1359 (2019).

71. Smith, S. A. & Brown, J. W. Constructing a broadly inclusive seed plant phylogeny. *American Journal of Botany* **105**, 302–314 (2018).

72. Zanne, A. E. *et al.* Three keys to the radiation of angiosperms into freezing environments. *Nature* **506**, 89–92 (2014).

73. Qian, H. & Jin, Y. An updated megaphylogeny of plants, a tool for generating plant phylogenies and an analysis of phylogenetic community structure. *Journal of Plant Ecology* **9**, 233–239 (2016).

74. Revell, L. J. phytools: Phylogenetic Tools for Comparative Biology (and Other Things). (2023).

75. Letten, A. D. & Cornwell, W. K. Trees, branches and (square) roots: why evolutionary relatedness is not linearly related to functional distance. *Methods in Ecology and Evolution* **6**, 439–444 (2015).

76. de Bello, F., Carmona, C. P., Lepš, J., Szava-Kovats, R. & Pärtel, M. Functional diversity through the mean trait dissimilarity: resolving shortcomings with existing paradigms and algorithms. *Oecologia* **180**, 933–940 (2016).

77. Petchey, O. L. & Gaston, K. J. Extinction and the loss of functional diversity. *Proceedings of the Royal Society of London. Series B: Biological Sciences* **269**, 1721–1727 (2002).

78. Cadotte, M. W. *et al.* Phylogenetic diversity metrics for ecological communities: integrating species richness, abundance and evolutionary history. *Ecology Letters* **13**, 96–105 (2010).

79. Gotelli, N. J. & McCabe, D. J. Species Co-Occurrence: A Meta-Analysis of J. M. Diamond's Assembly Rules Model. *Ecology* **83**, 2091–2096 (2002).

80. Schultz, J. *The Ecozones of the World. The Ecological Division of the Geosphere*. *The Ecozones of the World: The Ecological Divisions of the Geosphere* 252 (2005). doi:10.1007/3-540-28527-X.

81. Karger, D. N. *et al.* Climatologies at high resolution for the earth's land surface areas. *Scientific Data* **4**, 170122 (2017).

82. Karger, D. N. *et al.* Data from: Climatologies at high resolution for the earth's land surface areas. 7266827510 bytes Dryad https://doi.org/10.5061/DRYAD.KD1D4 (2018).

83. Brown, S. C., Wigley, T. M. L., Otto-Bliesner, B. L. & Fordham, D. A. StableClim, continuous projections of climate stability from 21000 BP to 2100 CE at multiple spatial scales. *Sci Data* **7**, 335 (2020).

84. Renssen, H. & Isarin, R. F. B. The two major warming phases of the last deglaciation at ∼14.7 and ∼11.5 ka cal BP in Europe: climate reconstructions and AGCM experiments. *Global and Planetary Change* **30**, 117–153 (2001).

85. Hijmans, R. J. *Raster: Geographic Data Analysis and Modeling*. (2023).

86. Wood, S. mgcv: Mixed GAM Computation Vehicle with Automatic Smoothness Estimation. (2023).

87. Wood, S. N. Fast stable restricted maximum likelihood and marginal likelihood estimation of semiparametric generalized linear models. *Journal of the Royal Statistical Society (B)* **73**, 3–36 (2011).

88. Wood, S. N. Stable and efficient multiple smoothing parameter estimation for generalized additive models. *Journal of the American Statistical Association* **99**, 673–686 (2004).

89. Wood, S. N. *Generalized Additive Models: An Introduction with R*. (Chapman and Hall/CRC, 2017).

90. Wood, S. N. Thin-plate regression splines. *Journal of the Royal Statistical Society (B)* **65**, 95–114 (2003).

91. Wood, S. N., Pya, N. & Säfken, B. Smoothing Parameter and Model Selection for General Smooth Models. *Journal of the American Statistical Association* **111**, 1548–1563 (2016).

92. Hijmans, R. J., Phillips, S., Leathwick, J. & Elith, J. *Dismo: Species Distribution Modeling*. (2022).

93. Arel-Bundock, V. *Marginaleffects: Predictions, Comparisons, Slopes, Marginal Means, and Hypothesis Tests*. (2023).

94. R Core Team. *R: A Language and Environment for Statistical Computing*. (R Foundation for Statistical Computing, Vienna, Austria, 2022).

95. Hähn, G. J. A., Damasceno, G., Sabatini, F. M., & Bruelheide, H. (2024). Global decoupling of functional and phylogenetic diversity in plant communities (Version 1.0) [Dataset]. German Centre for Integrative Biodiversity Research. https://doi.org/10.25829/idiv.3574-mpmk21